

Geophysical Research Letters®

RESEARCH LETTER

10.1029/2022GL100215

Key Points:

- Ocean heat uptake efficiency (OHUE) change is estimated from ocean heat content and global mean surface temperature records
- There is a >99% probability that ocean heat uptake efficiency increased over the past five decades
- OHUE was on average $0.58 \pm 0.08 \text{ W/m}^2\text{K}$ over this period and increased during it by $0.19 \pm 0.04 \text{ W/m}^2\text{K}$

Correspondence to:

B. B. Cael,
cael@noc.ac.uk


Citation:

Cael, B. B. (2022). Ocean heat uptake efficiency increase since 1970. *Geophysical Research Letters*, 49, e2022GL100215. <https://doi.org/10.1029/2022GL100215>

Received 28 JUN 2022
Accepted 21 SEP 2022

© 2022. The Authors.
This is an open access article under the terms of the [Creative Commons Attribution License](#), which permits use, distribution and reproduction in any medium, provided the original work is properly cited.

Ocean Heat Uptake Efficiency Increase Since 1970

B. B. Cael¹ 

¹National Oceanography Centre, Southampton, UK

Abstract The ocean stores the bulk of anthropogenic heat in the Earth system. The ocean heat uptake efficiency (OHUE)—the flux of heat into the ocean per degree of global warming—is therefore a key factor in how much warming will occur in the coming decades. In climate models, OHUE is well-characterized, tending to decrease on centennial timescales; in contrast, OHUE is not well-constrained from Earth observations. Here OHUE and its rate of change are diagnosed from global temperature and ocean heat content records. OHUE increased over the past five decades by $0.19 \pm 0.04 \text{ W/m}^2\text{K}$, and was on average $0.58 \pm 0.08 \text{ W/m}^2\text{K}$ during this period. This increase is attributed to steepening anthropogenic heat gradients in the ocean, and corresponds to several years' difference in when temperature targets such as 1.5 or 2°C are exceeded.

Plain Language Summary Human activity causes extra energy to be radiated back onto Earth's surface. Much of this extra energy accumulates in the ocean as heat. Based on records of global warming and the ocean's heat content, here it is shown that the *efficiency* of the transfer of this energy into the ocean has increased in recent decades. This “ocean heat uptake efficiency” is the amount of energy transferred into the ocean per degree of global warming, and has increased by roughly a third over the past five decades. This translates into several years' delay until global warming temperature targets, such as 2°C warming, are exceeded.

1. Introduction

Global warming can be understood in terms of conservation of energy of the Earth's surface. The amount of warming corresponds to the difference between the extra energy radiated to the Earth's surface via anthropogenic and natural factors, that is, the radiative forcing, versus the amount of that energy that is exported elsewhere (Sellers, 1969). A key reservoir for the export of this excess energy is the ocean, which contains almost all of the anthropogenic heat in the Earth system (Cheng, 2022; Cheng et al., 2017; Domingues et al., 2008; JMA., 2022; Levitus et al., 2012). This ocean heat content (OHC H , [$ZJ = 10^{21}J$]) has increased by hundreds of zetajoules over the past several decades of sustained ocean observations, during which time Earth's global mean surface temperature anomaly (T , [K]) has increased by about 1°C (Cowtan & Way, 2014; Hansen et al., 2006; Hersbach et al., 2020; Lindsey & Dahllman, 2020; Morice et al., 2021; Rohde & Hausfather, 2020).

More important than OHC for future climate change is the ocean heat uptake *efficiency* (OHUE, κ [$\text{W/m}^2 \text{K}$], Materials and Methods (MM)) (Gregory & Mitchell, 1997; Newsom et al., 2020), that is, how much energy Earth's surface exports downwards into the ocean per degree of global warming. κ is thus an integrated metric of the climate system's capacity to “resist” surface warming by fluxing excess energy (i.e., anthropogenic heat) into the ocean, and is determined by numerous factors including the surface pattern of warming (Armour et al., 2013; Newsom et al., 2020; Rose et al., 2014) and the ocean circulation (Gregory et al., 2015; Watanabe et al., 2013; Winton et al., 2010). The impact of OHUE on global warming is most simply expressed via a metric sometimes referred to as the transient climate sensitivity (TCS [K], MM) (Padilla et al., 2011; Raper et al., 2002; Winton et al., 2010), which expresses the expected warming at the time that the atmospheric CO_2 concentration reaches double its pre-industrial level after decades of sustained anthropogenic emissions. TCS is defined as $\text{TCS} = F_{2\times\text{CO}_2}/(-\lambda + \kappa)$, where $F_{2\times\text{CO}_2}$ [W/m^2] is the radiative forcing associated with a doubling of the atmospheric CO_2 concentration from pre-industrial levels and λ [$\text{W/m}^2\text{K}$] is the climate feedback, which analogous to κ corresponds to how much energy Earth's surface exports upwards to space per degree of global warming (Sherwood et al., 2020) (n.b. the sign conventions of κ and λ are such that a negative and positive λ and κ stabilizes the climate). The larger the value of κ , the less warming is expected in coming decades.

OHUE is fairly well-characterized within Earth System Models (ESMs, including coupled atmosphere-ocean general circulation models). This is mostly via experiments where atmospheric CO_2 is increased by 1% per year

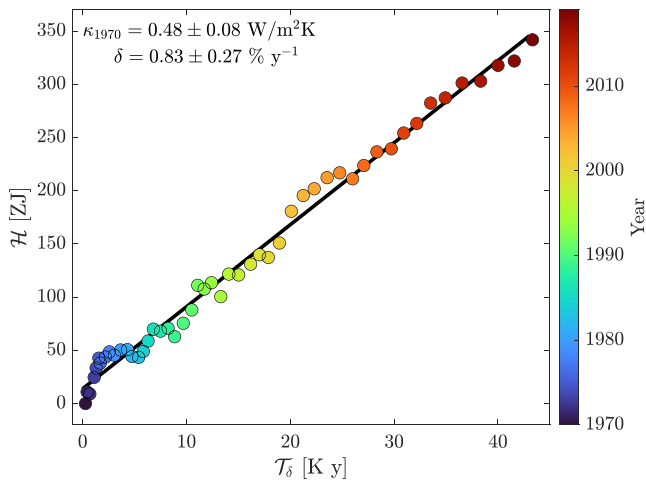


Figure 1. Illustration of regression of ocean heat content (H , [ZJ], ensemble median shown) versus weighted temperature integral (T_{δ} , [K y], ensemble median shown) to find initial ocean heat uptake efficiency (κ_{1970} , [W/m²K]) and rate of change (δ , [y⁻¹]).

for 70 years, after which time it has doubled; OHUE can then be defined as the ratio of H and T after about 70 years, for instance (Gregory & Mitchell, 1997; Kuhlbrodt & Gregory, 2012). Notably, when these experiments are run for 140 years to the point that atmospheric CO₂ quadruples, OHUE almost always decreases between ~70 and ~140 years, though by how much varies substantially between models (Gregory et al., 2015; Watanabe et al., 2013). While these scenarios are of limited use for describing real historical climatic changes, they are a core component of idealized understanding of OHUE.

In contrast, OHUE is poorly constrained for the real climate system, hindering efforts to validate ESMS' predictions of climate change in coming decades. Here a method is presented to diagnose OHUE from observations of ocean heat content and temperature alone (MM). OHUE significantly increased by 0.19 ± 0.04 W/m²K over the past five decades (>99% confidence). This is attributed to the steepening of anthropogenic heat gradients in the ocean, rather than ocean circulation changes, and corresponds to several years' delay in when the temperature targets laid out in the Paris Agreement are exceeded (Adoption of the Paris Agreement FCCC/CP/2015/L.9/Rev.1, 2015).

2. Results and Discussion

The method is described in detail in MM. Briefly, the OHC (H) is regressed against the integral of the time-weighted temperature anomaly \mathcal{T} [K y]; the slope of this regression corresponds to κ . An ensemble derived from the infilled HadCRUT5 (Morice et al., 2021) ensemble experiment is used for T , and an ensemble derived from the JMA (Ishii et al., 2017; JMA., 2022), Cheng (Cheng, 2022; Cheng et al., 2017), and NCEI (Domingues et al., 2008; Levitus et al., 2012) H products is used for H (MM). The years 1970–2019 are used because these are the years with enough signal relative to measurement uncertainties (MM). There is significant (probability >99%) positive curvature in the residuals of this regression (MM), indicating a time-evolution of κ . This is captured by an ansatz that κ changes linearly with time, from an initial value κ_{1970} [W/m²K], by a fixed amount $\delta\kappa_{1970}$ [W/m²Ky] each year. This ansatz is introduced by replacing \mathcal{T} with an integrated time-weighted temperature anomaly T_{δ} ; the best-fitting δ value for each temperature ensemble member is selected with its corresponding κ_{1970} to quantify uncertainty. The ansatz is then verified by the absence of curvature in the residuals of H regressed against T_{δ} (Figure 1). Thus, both the time-mean OHUE from the 1970s through the 2010s and the time evolution of OHUE, as approximated by a linear trend, are captured.

Figure 2 shows the joint distribution of the time-average OHUE, that is, the mean of κ , and the change in κ , that is, the final minus initial κ value, over this period. It is found that OHUE increased (i.e., $\delta > 0$, probability >99%) over the past five decades and that this increase is well-described as increasing with time rather than being a temperature-dependent effect (MM). The uncertainty in these two quantities is anticorrelated (Figure 2), such that the uncertainty in κ reduces slightly over time.

This trend corresponds to a fairly large relative change of $34 \pm 9\%$ in OHUE over the past five decades (Figure 3). This trend corresponds to an additional 113 ± 35 ZJ of heat stored in the ocean during this time period versus if OHUE stayed at its initial 1970 value, which is enough to heat the top ~45m of the ocean by 1°C, and $29 \pm 9\%$ of the total OHC accumulated during this time period. This trend also has appreciable consequences for near-term warming. Using standard values of $F_{2xCO_2} = 4 \pm 0.3$ W/m² and $\lambda = -1.3 \pm 0.44$ W/m² K (Sherwood et al., 2020), under a scenario where atmospheric CO₂ increases by 1% a year, a κ like that diagnosed for 1970 results in the exceeding 1.5°C (2°C) warming by 5.0 ± 1.2 years (6.7 ± 1.5 years) earlier than a κ like that diagnosed for 2019. While these calculations are based on the heuristic

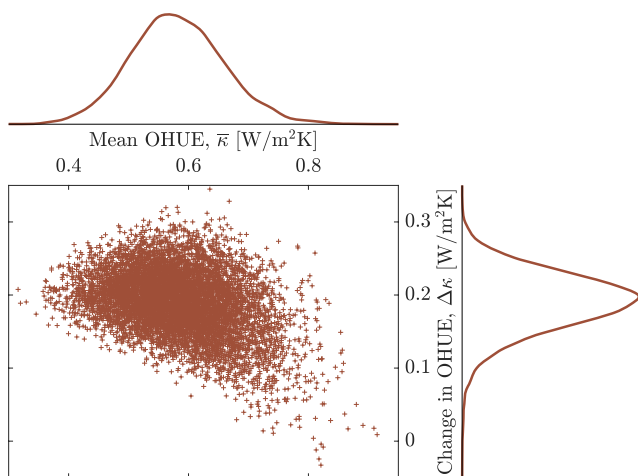


Figure 2. Joint distribution of time-mean ocean heat uptake efficiency ($\bar{\kappa}$, [W/m²K]) and change in ocean heat uptake efficiency ($\Delta\kappa$, [W/m²K]) from 1970 to 2019. Y-axes of top and right-hand side plots are probability densities with units the inverse of those on the corresponding X-axes.

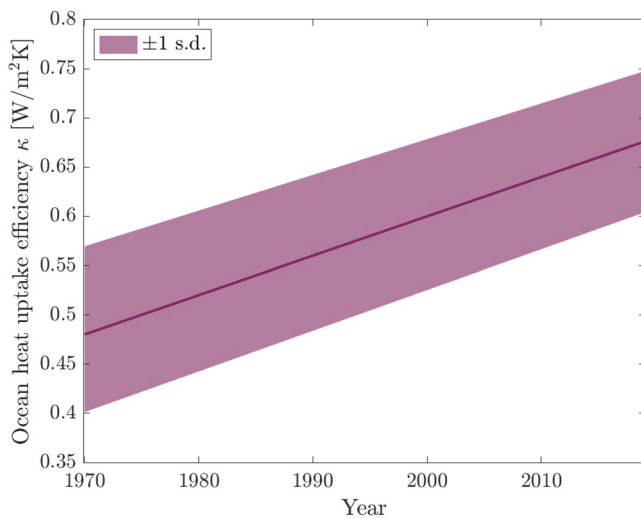


Figure 3. Ocean heat uptake efficiency κ , [W/m² K] versus time.

metric of TCS, they still nonetheless underscore an appreciable evolution of κ diagnosed here in terms of climate policy and projection. This difference will of course be even greater if the increase in κ continues, with opposite implications if the trend reverses in the near future. The numbers in this paragraph are intended to be illustrative of the implications of a positive trend in OHUE; all are uncertain stemming from the similar uncertainty in δ , and the sign of each of these holds with the same >99% confidence.

The likely increase in OHUE over the past five decades is attributed to the steepening of anthropogenic heat gradients over this time period as anthropogenic heat is accumulated in the ocean. Heat is primarily stored in the ocean in (a) the Southern Ocean and (b) the North Atlantic Ocean due to the overturning circulation, and (c) via stirring and mixing of gradients by eddies and other forms of ocean turbulence (Morrison et al., 2013). The increase in OHUE cannot be due to the first two of these, principally because the overturning circulation in neither the Southern Ocean nor the North Atlantic Ocean has not yet shown a definite systemic strengthening over this time period in observations (Kilbourne et al., 2022; Meredith et al., 2012). In contrast, the gradients of anthropogenic heat in the ocean have steadily increased over this time period as heat is continually injected into the upper ocean and comparatively slowly diffused into its interior (Cheng, 2022;

Cheng et al., 2017). Analogous to Fick's first law of diffusion, the steeper the gradients of anthropogenic heat, the more efficiently ocean turbulent processes can act to transport heat away from the surface. This results in a larger OHUE, because every additional amount of heat added to the surface ocean can be more easily transported into the ocean interior as these gradients steepen. This is also visible in the increased fraction of total OHC contained in deeper layers of the ocean over time (Cheng, 2022; Cheng et al., 2017). The change in κ is thus a result of passive transport of heat by ocean dynamics, rather than by the direct influence of the injected heat on the ocean's dynamics. This also explains why the change in κ is better explained as a temporal evolution than a temperature-dependent climate feedback, as its change is due to the steady steepening of these gradients.

As this is a generic phenomenon, the increase in OHUE over time is expected to continue in the near future, as anthropogenic heat gradients should continue to steepen in the ocean. Note that no evidence for a reversal of this increasing trend is observable in the residuals of the regression in Figure 1. However, it is important to note that this multidecadal increase in κ is not in disagreement with the centennial-scale decrease in κ observed in ESMs, which is thought to be due to the equilibration of the deep ocean with Earth's surface, that is, the eventual smoothing out of anthropogenic heat gradients (Gregory et al., 2015; Watanabe et al., 2013) and may also be a result of, not a response to future circulation changes. Even under sustained radiative forcing, the deep ocean should eventually accumulate enough heat to weaken these anthropogenic heat gradients and OHUE should therefore decrease, as found in ESM experiments. ESMs should however be able to replicate this multidecadal increase in κ , though they are expected to reach an equilibrium temperature (corresponding to the equilibrium climate sensitivity) at some point after radiative forcing is stabilized. It is likely possible however that 140 years is too fast a timescale to expect the deep ocean to equilibrate with Earth's surface under sustained emissions. It would be instructive to investigate the centennial κ behavior within ESMs that can resolve the multidecadal increasing trend in κ diagnosed from observations here. OHUE may also decrease over time due to overturning circulation changes that have not yet occurred.

Altogether these results demonstrate the importance of deriving observational estimates of the key climate parameters that determine the Earth's response to anthropogenic forcing, as well as the evolution of these parameters over time, as critical counterpoints to ESM estimates both to evaluate models and to make independent projections. It would be most instructive to apply the method presented here to large ensembles of historical simulations as an indicator of model performance. That said, the method assumes a linear trend over the entire period, which is effective for finding an average change over time and justified by the lack of curvature in the residuals, but necessarily misses whether this trend may have reversed at some point or been confined to particular periods. Finally, the method presented here is a simple statistical diagnosis of changes in, and time-mean, OHUE, relying only on surface temperature and ocean heat content records; it therefore cannot distinguish how different forcing

agents such as anthropogenic aerosols or volcanic eruptions, nor different modes of climate variability such as the El Niño Southern Oscillation, influence OHUE. It also cannot distinguish the extent to which diagnosed trends are due to or modulated by natural climate variability. Understanding the influence of such factors is an important part of utilizing this observational diagnosis to evaluate ESMs.

3. Materials and Methods

Theory: The flux of energy from the Earth's surface boundary layer into the ocean H [ZJ/year] can be integrated from an initial time point t_i to yield the ocean heat content anomaly $\mathcal{H}(t)$ [ZJ]:

$$\mathcal{H}(t) = \int_{t_i}^t H(\tau) d\tau$$

where τ is a dummy variable. The ocean heat content efficiency κ [ZJ/K y] is defined as this energy flux per degree of global warming, that is, $\kappa = H/T$ so that

$$\mathcal{H}(t) = \int_{t_i}^t H(\tau) d\tau = \int_{t_i}^t \kappa(\tau)T(\tau) d\tau$$

The ansatz is then made that $\kappa = \kappa_i(1 + \delta(t - t_i))$, that is, κ starts at κ_i at t_i and increases by a constant amount $\delta\kappa_i$ each year— δ here is a number (in units of y^{-1}), not the Kronecker delta function. For simplicity t_i is redefined as year zero so $\kappa = \kappa_i(1 + \delta t)$; one can then substitute

$$\mathcal{H}(t) = \int_{t_i}^t \kappa_i(1 + \delta\tau)T(\tau) d\tau = \kappa_i \int_{t_i}^t (1 + \delta\tau)T(\tau) d\tau$$

The year 1970 is then redefined as the initial year and the initial ocean heat uptake efficiency is labeled as κ_{1970} for clarity. If one then defines

$$\mathcal{T}_\delta(t) = \int_{t_i}^t (1 + \delta\tau)T(\tau) d\tau$$

then the slope

$$\mathcal{H}(t)/\mathcal{T}_\delta(t) = \kappa_{1970}$$

If the ansatz is valid and the correct δ is selected, this δ will capture all the time-dependence of κ and this slope will be constant in time, that is, there will be no systematic behavior or curvature in the residuals of $\mathcal{H}(t)$ regressed against $\mathcal{T}_\delta(t)$. Finally for all figures, κ is divided by a factor of 16.09 to convert zetajoules per degree Kelvin per year to watts per square meter per second; this is the surface area of the Earth ($5.101 \times 10^{14} \text{ m}^2$) times the number of seconds in a year (3.154×10^7) divided by the number of joules in a zetajoule (10^{21}). Note that this is an average over the full Earth surface, not just the ocean surface, in keeping with the standard definition.

Temperature data: The HadCRUT5 temperature record is used here, which is provided as a 200 member ensemble. From this ensemble a 10,000 member ensemble is generated by calculating the estimated Gaussian covariance matrix based on the ensemble and simulating 10,000 members with the same covariance properties as the original ensemble. Repeating the analysis with the original 200 member ensemble yields effectively identical results. HadCRUT5 is described in detail in (Morice et al., 2021). $T(t)$ [K] is defined as the temperature anomaly vs. the 1850–1900 average. This temperature record is selected because (a) uncertainties being expressed as ensemble members makes the propagation of uncertainty straightforward when integrating in time, and (b) the HadCRUT5 ensemble captures the uncertainty across temperature time series. Specifically, when 0.03 K is subtracted from the $T(t)$ ensemble, 99% of the temperatures across all years of five other temperature products (Cowtan & Way, 2014; Hansen et al., 2006; Hersbach et al., 2020; Lindsey & Dahlman, 2020; Rohde & Hausfather, 2020) are above (below) the first (99th) percentile of the ensemble. This value of 0.03 K is not subtracted from the ensemble for the calculations herein, but subtracting it does not change the results.

Ocean heat content data: The Japanese Meteorological Agency (Ishii et al., 2017; JMA., 2022), Cheng (Cheng, 2022; Cheng et al., 2017), and National Centers for Environmental Information (Domingues et al., 2008; Levitus et al., 2012) ocean heat content records are used here, which are provided as ocean heat content over 0–2,000 m. A 10,000 member ensemble is generated from these by calculating the estimated Gaussian covariance matrix from the three time-series and simulating ensemble members with the same covariance properties. The ensemble thus accounts for the across-product uncertainties. The time series are described in detail in the above citations; the values were taken from the links given in the Acknowledgments. $\mathcal{H}(t)$ [ZJ] is defined as the ocean heat content anomaly; the reference year is immaterial for the analysis here as only changes over time affect the parameters. Reanalysis products are not considered because these “are not suitable for studies of long-term trends or low frequency variability across data-sparse time periods” (Killick & Atmospheric Research Staff, 2020). Years 1970–2019 are considered because (a) both ocean heat content and temperature increase very little prior to 1970 compared with uncertainty and interannual variability, and ocean heat content in particular before 1970 is very uncertain and sparsely observed, and (b) all three observational ocean heat content products are available for comparison to generate an across-product ensemble up to 2019.

Initial curvature calculation: Time-evolution of κ (i.e., $\delta \neq 0$) is tested for initially by regressing $\mathcal{H}(t)$ versus each ensemble member of $\mathcal{T}_{\delta=0}(t)$. A quadratic regression is performed. For >99% of these regressions the quadratic term is positive, indicating that δ is significantly positive and necessary to describe the relationship between T and \mathcal{H} .

Primary analysis: To generate an estimate of κ_{1970} and δ , for each $T(t)$ ensemble member, the following procedure is followed: (a) sample a large range of δ values (in practice the range -0.005 to 0.02 y^{-1} at 0.0001 resolution is sufficient; see Figure 2), (b) calculate $\mathcal{T}_{\delta}(t)$ for each, (c) perform a linear regression of $\mathcal{H}(t)$ against $\mathcal{T}_{\delta}(t)$ for each, (d) select the δ value for which the linear regression has the lowest residual sum of squares (or equivalently the highest r^2 or equivalently the lowest root-mean-square error). The associated κ_{1970} is the slope of this δ 's linear regression (Figure 1). These δ values yielded linear relationships between $\mathcal{H}(t)$ and $\mathcal{T}_{\delta}(t)$; the quadratic term in a quadratic regression analogous to that described for the $\delta = 0$ case was $< 1z$ -score different from zero for all ensemble members.

Temperature versus time analysis: The evolution of κ as a function of time is compared to that of a temperature-dependent κ , that is, the ansatz $\kappa = \kappa_{1970}(1 + \delta T)$ is compared to the ansatz $\kappa = \kappa_{1970}(1 + \delta t)$ in the main text. A temperature-dependent κ would correspond to a type of temperature-dependent climate feedback, whereby the climate sensitivity depends on the temperature itself (Bloch-Johnson et al., 2021). The above analysis is repeated with the alternative ansatz to evaluate which model has the higher r^2 (or equivalently the lower residual sum of squares or equivalently the lower root-mean-square error); in 82% instances this is the time-dependent model, indicating the ansatz in the text is a better description of the evolution of κ than a temperature-dependent κ .

Years to 1.5 or 2°C: To estimate the difference in years taken to surpass 1.5 or 2°C, the transient climate sensitivity $TCS = F_{2\times CO_2} / (-\lambda + \kappa)$ is calculated, where $F_{2\times CO_2} = N(4.0, 0.3) \text{ W/m}^2$ is the radiative forcing associated with a doubling of CO_2 and $\lambda = N(-1.3, 0.44) \text{ W/m}^2\text{K}$ is the climate feedback (Sherwood et al., 2020). Note that the TCS is closely related to the arguably more relevant metric of the transient climate response (Winton et al., 2010); the TCS is preferred in this context, however, as the TCR would require a specification of the surface boundary layer's heat capacity, a term that is less certain than those that comprise the TCS. The TCS analysis is equivalent to TCR under the plausible assumption that the surface boundary layer's heat capacity is small on the order of 30 ZJ or less, equivalent to roughly the top 10 m of the global ocean. The year of crossing a temperature threshold of C degrees is then defined as $y = 70C/TCS$; 70 is the number of years that is required for atmospheric CO_2 concentrations to increase at 1% per year until the concentration doubles, which corresponds to a linear increase in radiative forcing under the assumption of logarithmic CO_2 forcing (Bloch-Johnson et al., 2021). For each (κ_{1970}, δ) pair, a random value of $F_{2\times CO_2}$ and λ are sampled from the distributions above, and y is calculated for $C = 1.5$ and 2°C , and for κ_{1970} and $\kappa_{2019} = \kappa_{1970}(1 + 49\delta)$. The difference $y(C = 2, \kappa_{2019}) - y(C = 2, \kappa_{1970})$ is 6.7 ± 1.5 years; the difference $y(C = 1.5, \kappa_{2019}) - y(C = 1.5, \kappa_{1970})$ is 5.0 ± 1.2 years. Note that this is a heuristic metric and is only intended to illustrate the potential impact of the change in κ diagnosed herein. It is emphasized that no extrapolation of the observed trend is used here; only the initial and final κ values are compared, and are applied as time-invariant quantities.

Conflict of Interest

The authors declare no conflicts of interest relevant to this study.

Data Availability Statement

The data on which this article is based are available at <https://www.metoffice.gov.uk/hadobs/hadcrut5/data/current/download.html>, https://www.data.jma.go.jp/gmd/kaiyou/english/ohc/ohc_data_en.html, <http://159.226.119.60/cheng/>, and <https://www.ncei.noaa.gov/access/global-ocean-heat-content/index.html>. Code is available at <https://doi.org/10.5281/zenodo.7115765>.

Acknowledgments

It is a pleasure to thank the many scientists whose collective work has generated the time series on which this work relies. This work was supported by the National Environmental Research Council through ECOMAD (Enhancing Climate Observations, Models and Data) and by the European Union's Horizon 2020 Research and Innovation Programme under grant agreement No. 820989 (project COMFORT). The work reflects only the authors' view; the European Commission and their executive agency are not responsible for any use that may be made of the information the work contains. Cael conceived the study, performed the analyses, and wrote the paper.

References

- Adoption of the Paris Agreement FCCC/CP/2015/L.9/Rev.1. (2015). UNFCCC.
- Armour, K. C., Bitz, C. M., & Roe, G. H. (2013). Time-varying climate sensitivity from regional feedbacks. *Journal of Climate*, 26(13), 4518–4534. <https://doi.org/10.1175/jcli-d-12-00544.1>
- Bloch-Johnson, J., Rugenstein, M., Stolpe, M. B., Rohrschneider, T., Zheng, Y., & Gregory, J. M. (2021). Climate sensitivity increases under higher CO₂ levels due to feedback temperature dependence. *Geophysical Research Letters*, 48(4), e2020GL089074. <https://doi.org/10.1029/2020gl089074>
- Cheng, L. (2022). OHC by IAP, Retrieved from <http://159.226.119.60/cheng/>
- Cheng, L., Trenberth, K. E., Fasullo, J., Boyer, T., Abraham, J., & Zhu, J. (2017). Improved estimates of ocean heat content from 1960 to 2015. *Science Advances*, 3(3), e1601545. <https://doi.org/10.1126/sciadv.1601545>
- Cowan, K., & Way, R. G. (2014). Coverage bias in the HADCRUT4 temperature series and its impact on recent temperature trends. *Quarterly Journal of the Royal Meteorological Society*, 140(683), 1935–1944. <https://doi.org/10.1002/qj.2297>
- Domingues, C. M., Church, J. A., White, N. J., Gleckler, P. J., Wijffels, S. E., Barker, P. M., & Dunn, J. R. (2008). Improved estimates of upper-ocean warming and multi-decadal sea-level rise. *Nature*, 453(7198), 1090–1093. <https://doi.org/10.1038/nature07080>
- Gregory, J. M., Andrews, T., & Good, P. (2015). The inconstancy of the transient climate response parameter under increasing CO₂. *Philosophical Transactions of the Royal Society A: Mathematical, Physical and Engineering Sciences*, 373(2054), 20140417. <https://doi.org/10.1098/rsta.2014.0417>
- Gregory, J. M., & Mitchell, J. F. (1997). The climate response to CO₂ of the Hadley Centre coupled AOGCM with and without flux adjustment. *Geophysical Research Letters*, 24(15), 1943–1946. <https://doi.org/10.1029/97gl01930>
- Hansen, J., Ruedy, R., Sato, M., & Lo, K. (2006). NASA GISS surface temperature (GISTEMP) analysis. *Trends: A Compendium of Data on Global Change*.
- Hersbach, H., Bell, B., Berrisford, P., Hirahara, S., Horányi, A., & Muñoz-Sabater, J. (2020). The ERA5 global reanalysis. *Quarterly Journal of the Royal Meteorological Society*, 146(730), 1999–2049.
- Ishii, M., Fukuda, Y., Hirahara, S., Yasui, S., Suzuki, T., & Sato, K. (2017). Accuracy of global upper ocean heat content estimation expected from present observational data sets. *Sola*, 13(0), 163–167. <https://doi.org/10.2151/sola.2017-030>
- JMA. (2022). JMA's global ocean heat content data, Retrieved from https://www.data.jma.go.jp/gmd/kaiyou/english/ohc/ohc_data_en.html
- Kilbourne, K. H., Wanamaker, A. D., Moffa-Sanchez, P., Reynolds, D. J., Amrhein, D. E., Butler, P. G., et al. (2022). Atlantic circulation change still uncertain. *Nature Geoscience*, 15(3), 165–167. <https://doi.org/10.1038/s41561-022-00896-4>
- Killick, R., & Atmospheric Research Staff. (2020). The climate data guide. In *EN4 subsurface temperature and salinity for the global oceans*. Retrieved from <https://climatedataguide.ucar.edu/climate-data/en4-subsurface-temperature-and-salinity-global-oceans>
- Kuhlbrodt, T., & Gregory, J. (2012). Ocean heat uptake and its consequences for the magnitude of sea level rise and climate change. *Geophysical Research Letters*, 39(18). <https://doi.org/10.1029/2012gl052952>
- Levitus, S., Antonov, J. I., Boyer, T. P., Baranova, O. K., Garcia, H. E., & Locarnini, R. A. (2012). World ocean heat content and thermocline sea level change (0–2,000 m). *Geophysical Research Letters*, 39(10), 1955–2010. <https://doi.org/10.1029/2012GL051106>
- Lindsey, R., & Dahlman, L. (2020). Climate change: Global temperature. *Climate Gov*, 16.
- Meredith, M. P., Garabato, N., Hogg, A. M., & Farneti, R. (2012). Sensitivity of the overturning circulation in the southern ocean to decadal changes in wind forcing. *Journal of Climate*, 25(1), 99–110. <https://doi.org/10.1175/2011jcli4204.1>
- Morice, C. P., Kennedy, J. J., Rayner, N. A., Winn, J., Hogan, E., Killick, R., et al. (2021). An updated assessment of near-surface temperature change from 1850: The HADCRUT5 data set. *Journal of Geophysical Research: Atmosphere*, 126(3), e2019JD032361. <https://doi.org/10.1029/2019jd032361>
- Morrison, A., Saenko, O., Hogg, A. M., & Spence, P. (2013). The role of vertical eddy flux in southern ocean heat uptake. *Geophysical Research Letters*, 40(20), 5445–5450. <https://doi.org/10.1002/2013gl057706>
- Newsom, E., Zanna, L., Khatiwala, S., & Gregory, J. M. (2020). The influence of warming patterns on passive ocean heat uptake. *Geophysical Research Letters*, 47(18), e2020GL088429. <https://doi.org/10.1029/2020gl088429>
- Padilla, L. E., Vallis, G. K., & Rowley, C. W. (2011). Probabilistic estimates of transient climate sensitivity subject to uncertainty in forcing and natural variability. *Journal of Climate*, 24(21), 5521–5537. <https://doi.org/10.1175/2011jcli3989.1>
- Raper, S. C., Gregory, J. M., & Stouffer, R. J. (2002). The role of climate sensitivity and ocean heat uptake on AOGCM transient temperature response. *Journal of Climate*, 15(1), 124–130. [https://doi.org/10.1175/1520-0442\(2002\)015<0124:trocsa>2.0.co;2](https://doi.org/10.1175/1520-0442(2002)015<0124:trocsa>2.0.co;2)
- Rohde, R. A., & Hausfather, Z. (2020). The Berkeley Earth land/ocean temperature record. *Earth System Science Data*, 12(4), 3469–3479. <https://doi.org/10.5194/essd-12-3469-2020>
- Rose, B. E., Armour, K. C., Battisti, D. S., Feldl, N., & Koll, D. D. (2014). The dependence of transient climate sensitivity and radiative feedbacks on the spatial pattern of ocean heat uptake. *Geophysical Research Letters*, 41(3), 1071–1078. <https://doi.org/10.1002/2013gl058955>
- Sellers, W. D. (1969). A global climatic model based on the energy balance of the Earth-atmosphere system. *Journal of Applied Meteorology and Climatology*, 8(3), 392–400. [https://doi.org/10.1175/1520-0450\(1969\)008<0392:agcmbo>2.0.co;2](https://doi.org/10.1175/1520-0450(1969)008<0392:agcmbo>2.0.co;2)

- Sherwood, S., Webb, M. J., Annan, J. D., Armour, K. C., Forster, P. M., Hargreaves, J. C., et al. (2020). An assessment of Earth's climate sensitivity using multiple lines of evidence. *Reviews of Geophysics*, 58(4), e2019RG000678. <https://doi.org/10.1029/2019rg000678>
- Watanabe, M., Kamae, Y., Yoshimori, M., Oka, A., Sato, M., Ishii, M., & Kimoto, M. (2013). Strengthening of ocean heat uptake efficiency associated with the recent climate hiatus. *Geophysical Research Letters*, 40(12), 3175–3179. <https://doi.org/10.1002/grl.50541>
- Winton, M., Takahashi, K., & Held, I. M. (2010). Importance of ocean heat uptake efficiency to transient climate change. *Journal of Climate*, 23(9), 2333–2344.